The Transition from Free to Forced Convection in Mass Transfer from Solid Spheres

F. H. GARNER and J. M. HOFFMAN

University of Birmingham, Birmingham, England

Mass transfer rates have been measured at 30°C. over a Reynolds number range of 1 to 130 for the solution of ⅜-in. diameter spheres of benzoic acid for both upflow and downflow streams. These are compared with similar results for ¾-in. diameter spheres and show a gradual transition from forced to free convection. The interaction between the two effects is complex but less marked for the smaller spheres. Free convective effects do not disappear entirely until a Reynolds number of about 250 for the ⅜-in. spheres, compared with a value of 750 given for ¾-in. spheres in the previous work (6).

Mass transfer rates at low water flows from benzoic acid spheres of ¾-in. diameter have already been measured to investigate the transition from forced to free convection (*6*). It was decided to measure mass transfer rates for ⅜-in. diameter spheres in order to confirm the previous work and also to find the effect of varying the Rayleigh number.

THEORY

Krischer and Loos (*9, 10*) suggested the use of an equivalent Reynolds number $N_{Re}{}^{+}$ for the correlation of data in the region where free and forced convection are both important. This equivalent Reynolds number is derived as follows.

In the Grashof number the group $d(\Delta\rho)/(\rho)$ represents the buoyancy potential energy. For frictionless flow this can be replaced by a maximum kinetic energy of $W^2_{max}/2g$, and thus by definition

$$N'_{Gr} = \frac{1}{2} \cdot \frac{d^2 W^2{}_{max}}{2} = \frac{1}{2} N^2{}_{Re_w\ max} \qquad (1)$$

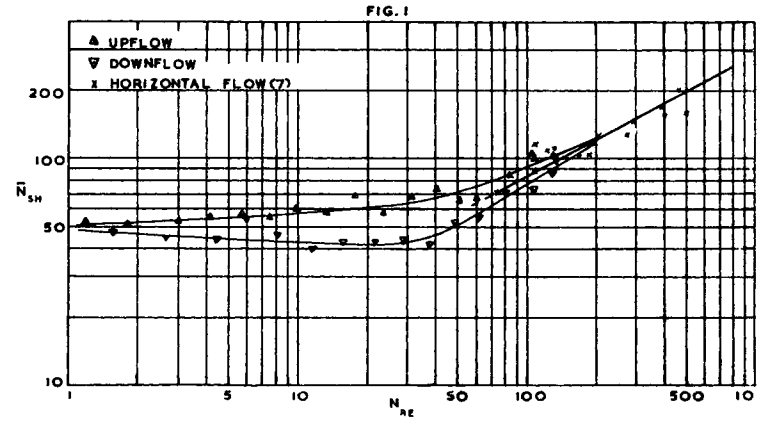

Fig. 1. Over-all mass transfer rates for ⅜-in. diameter spheres.

Then by making the assumption that free and forced convection are additive, the equivalent Reynolds number is

$$N_{Re}{}^{+} = N_{Re} + \sqrt{2\,N'_{Gr}} \qquad (2)$$

A more fundamental approach was suggested by Acrivos (*1*). The Navier Stokes equation and Fick's second law for transfer from a sphere, simplified by the normal assumptions of boundary layer theory, may be put into the following dimensionless form by suitable substitutions:

$$\left.\begin{aligned} &u_1 \frac{\partial u_1}{\partial x_1} + v_1 \frac{\partial u_1}{\partial y_1} = \pm \frac{N'_{Gr}}{N^2_{Re}} \sin\epsilon + u \frac{du}{dx_1} + \frac{\partial^2 u_1}{\partial y_1{}^2} \\ &\frac{\partial p_1}{\partial y_1} = 0 \\ &\frac{\partial (r_1 u_1)}{\partial x_1} + \frac{\partial (r_1 v_1)}{\partial y_1} = 0 \\ &u_1 \frac{\partial \eta}{\partial x_1} + v_1 \frac{\partial \eta}{\partial y_1} = \frac{1}{N_{Sc}} \frac{\partial^2 \eta}{\partial y_1{}^2} \end{aligned}\right\} \qquad (3)$$

where

$$u_1 = \frac{u}{U_o} \quad v_1 = \frac{v}{U_o} N_{Re}^{1/2}$$

$$x_1 = \frac{x}{d} \quad y_1 = \frac{y}{d} N_{Re}^{1/2}$$

$$p_1 = \frac{p}{\rho U_o^2} \quad r_1 = \frac{r}{d}$$

$$\eta = \frac{c - c_o}{c_s - c_o} \quad U = \frac{U^x}{U_o} \qquad (4)$$

The buoyancy term in the first equation will be positive when the flow and gravitation forces act in the same direction and negative when they oppose.

The boundary conditions are

$$y_1 = o \;\; u_1 = v_1 = o \;\; \eta = 1$$
$$y = \delta \;\; u_1 = U_{(e)_1} \;\; \eta = o \qquad (5)$$

For a given surface geometry the only parameters in the system of Equations (3) and (5) are N_{Sc}, $(N'_{Gr})/(N^2_{Re})$, and x_1. Thus the expression for the Sherwood number is

$$N_{Sh} = \frac{K_L d}{D} = N_{Re}^{1/2} \left(\frac{\partial \eta}{\partial y_1}\right)_{y_1=o}$$

$$= N_{Re}^{1/2} f\left(N_{Sc}, \frac{N'_{Gr}}{N^2_{Re}}, x_1\right) \qquad (6)$$

The over-all transfer rate may now be obtained by integrating Equation (6) with respect to x_1 from the forward stagnation point to some point which should not be beyond the position of separation of forward flow. This gives

$$\overline{N}_{Sh} = N_{Re}^{1/2} f\left(N_{Sc}, \frac{N'_{Gr}}{N^2_{Re}}\right) \qquad (7)$$

which should be useful for correlation purposes.

Acrivos (*1*) completed this solution by a numerical method for the heating and cooling of upward flow past a vertical plate. It was found that the transition from forced to free convection is gradual, especially at high Prandtl numbers, and that the two effects are nonadditive. The influence of free convection on the position of separation of forward flow was examined, and the solutions as $(N_{Gr})/(N^2_{Re}) \to \infty$ and $N_{Gr}/N^2_{Re} \to 0$ were compared with exact solutions and found to be in good agreement. The group N_{Gr}/N^2_{Re} also emerges in an analysis of heat transfer in vertical tubes at low Reynolds numbers given by Hanratty et al (*8*).

METHOD

The apparatus was essentially the same as that used earlier (*6*). It consisted of a double-ended vertical water tunnel of 6-in. I. D., designed to give streamline flow with a parabolic velocity distribution at the central test section for all flow rates used. The diameter of the column was considered large enough to make wall effects negligible. The only modification was that the 1-in. diameter recirculating pipe was lagged. This was an attempt to bring the temperature control for downflow in line with that for upflow, particularly at low flow rates. The method of operation was described in the earlier paper, and the controllability of flow rate and temperature, measured by their average standard deviations, was

flow rate	1.3%
temperature:	
(a) upflow	0.25°C.
(b) downflow.	0.23°C.

Diameter spheres ⅜-in. were made by compression of crystalline benzoic acid in a hand press. This gave spheres of high sphericity and uniformly high density:

upflow: average density = 1.296 g./cc. (99.5% solid density) σ = 0.0006 g./cc.

downflow: average density = 1.295 g./cc. (99.5% solid density). σ = 0.0007 g./cc.

Each sphere was supported at the rear stagnation point, since this gives the least disturbance in flow (*4*), the diameter of the support being 0.015 in. The spheres were photographed at the beginning and end of a test period. The negatives were projected giving a magnification of about 20x and the initial and final outlines of the sphere traced out. A small blob of solder on the support enabled the two to be superimposed in the correct position. The average diminution of radius was 0.0170 in. giving a probable error in measurement of about 6%. The diminution was measured at successive intervals of 10 deg. around the surface of the sphere, starting at the forward stagnation point, and local and over-all transfer coefficients were calculated.

The Reynolds number varied from 1 to 130, and all results were expressed on a constant Schmidt number basis (N_{Sc} = 788, temp. = 30°C.). The same data were used as were employed in the investigation of free convective mass transfer for benzoic acid in water (*5*).

RESULTS

Experimental observations and over-all and local mass transfer coefficients are given in Table 1.* The data af Garner and Suckling (*7*) for the dissolution of ⅜-in. diameter spheres of benzoic acid in water in horizontal flow are presented in Table 2.* These are recalculated to a constant Schmidt number basis both to allow for the different method used in the earlier paper to estimate diffusivity and to afford a useful comparison with the present work. These results for upflow, downflow, and horizontal flow are plotted in Figure 1, with $\overline{N}_{Sh}$ as ordinates vs. N_{Re} as abscissas. Local mass transfer rates at intervals of 30 deg. around the sphere surface have been plotted to give curves from which graphs of N_{Sh} vs. θ with N_{Re} as parameter have been drawn up for upflow (Figure 3) and downflow (Figure 4). Figure 2 is a plot of $\overline{N}_{Sh}$ against N_{Re} for the ⅜-in. spheres together with those obtained earlier for ¾-in. spheres (*6*).

DISCUSSION

Dimensional analysis of mass transfer shows that

$$N_{Sh} = f(N_{Re}, N_{Sc}, N'_{Gr})$$

In the region investigated all of these parameters are relevant, but for a series of runs with the same size of sphere and at constant temperature N_{Sc} and N'_{Gr} are constant. Thus it was decided to plot the results with $\overline{N}_{Sh}$ as ordinates against N_{Re} as absissae (Figure 1).

The results can be seen to have fallen on two smooth curves, one for upflow and one for downflow. There is a high degree of correlation with low mean probable errors:

FIG. 2

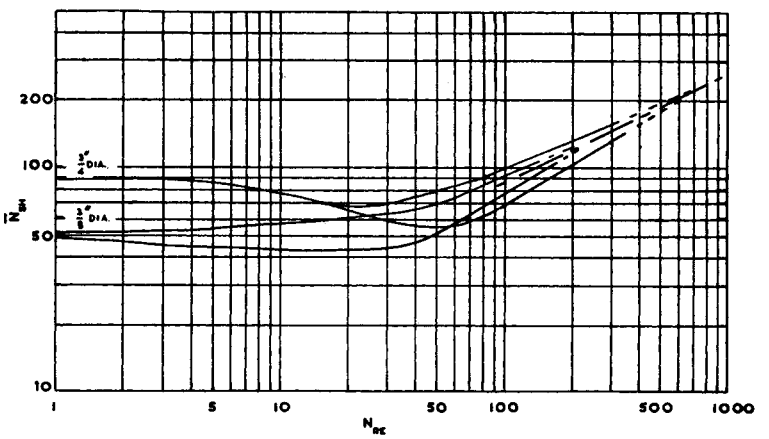

Fig. 2. Comparison of over-all mass transfer rates for ¾- and ⅜-in. diameter spheres.

* Tables 1 and 2 have been deposited as document 6382 with the American Documentation Institute, Photoduplication Service, Library of Congress, Washington 25, D. C., and may be obtained for $1.25 for photoprints or for 35-mm. microfilm.

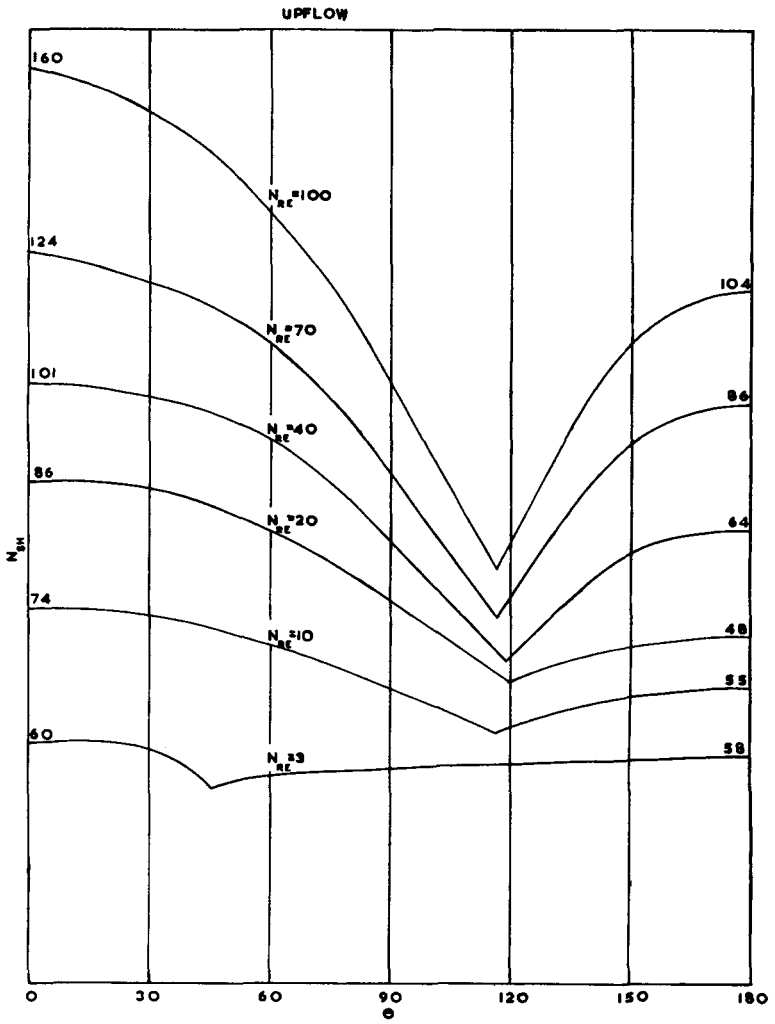

Fig. 3. Local mass transfer rates.

upflow: mean probable error = 4.4%
downflow: mean probable error = 4.9%

Since only one system was used, the major source of error will be in projection and measurement. The average diminution of radius was 0.0170-in., and this would give a probable error of 6%. Thus the results lie within the experimental error.

At very low Reynolds numbers (~ 1) the two curves approach each other and free convection is dominant. At higher Reynolds numbers the curve for upflow lies above that for downflow, and this separation is still apparent up to $N_{Re} = 200$. Such a separation has been noticed previously in the investigation of transfer in packed beds (3). Garner and Suckling's results (7) for the dissolution of ⅜-in. diameter spheres of benzoic acid in water in horizontal flow over the range $74 < N_{Re} < 520$ lie between these two curves. It is therefore justifiable to extrapolate the present curves to their upper point of intersection; this appears to be at a Reynolds number of about 250, and above this free convective transfer would seem to be insignificant. The curve for downflow appears to pass through a minimum at $N_{Re} \sim 25$, and although there is no perceptible minimum in the upflow curve, consideration of the plots of local mass transfer rates vs. N_{Re} with θ as parameter indicates the presence of one at $N_{Re} \sim 1.5$. Such a minimum was found to occur at $N_{Re} = 1$ by Bar-Ilan and Resnick (2) who studied the sublimation of napthalene spherules in air.

In Figure 2 the present work is compared with the results for the dissolution of ¾-in. diameter spheres of benzoic acid (6). This should indicate the effect of varying the Grashof number on the interaction between forced and free convection. For both sizes of sphere free convection is dominant at very low flow rates, but as the flow rate is increased the rate of mass transfer is depressed owing to interaction between forced and free convection. The depression is more marked for downflow than for upflow. On further increase in flow rate the mass transfer rate increases and tends towards that due to forced convection alone. Free convective effects do not disappear entirely until a Reynolds number of about 750 for the ¾-in. diameter spheres and 250 for the ⅜-in. diameter spheres. The minima in the curves for upflow and downflow are less pronounced for the smaller spheres and occur at lower Reynolds numbers than those for the larger spheres.

Sphere diam., in.	Direction of flow	N_{Re} at which minimum occurs	N_{Sh} min.
¾ in.	up	20	66
	down	45	54
⅜ in.	up	1.5	51
	down	25	43

This suggests that the maximum interaction between forced and free convection occurs when the two effects are of about the same magnitude and that interference is less the smaller the Rayleigh number. It can be seen that the two effects are nonadditive. This is in agreement with the theoretical predictions of Acrivos (1).

There is, however, a surprising aspect of these results. At very low flow rates ($N_{Re} \sim 1$) the curves for the ¾ and ⅜-in. spheres seem to be tending assymptotically towards Sherwood numbers of 88 and 50 respectively. These values might be expected to represent approximately the rate of transfer due to molecular diffusion and free convection alone, but in fact they are much higher than the values predicted from the work on free convection, which are 44.5 and 28.5 respectively (5). The difference can be ascribed neither to the experimental scatter of the low-speed work nor to that of the free convection. It is doubtful whether this is due to thermal convective currents, although there was probably a small vertical temperature gradient in the low speed water tunnel at low flows. On the other hand it can be seen from the experimental observations that temperature control at low flows is comparable with that at higher rates. It would seem then that, even at $N_{Re} = 1$, the flow in the 6-in. tunnel is great enough to sweep away solute from the outer edge of the boundary layer and this, combined with the nonuniform approach velocity to be expected under these conditions, is sufficient to give rates of transfer appreciably in excess of those due to free convection alone.

For completeness the results for both sphere sizes were correlated by the method suggested by Acrivos (1), that is by plotting $(N_{Sh})/(\sqrt{N_{Re}})$ against $(N'_{Gr})/(N_{Re}^2)$ at constant N_{Sc} (Figure 6). This gave two smooth curves for

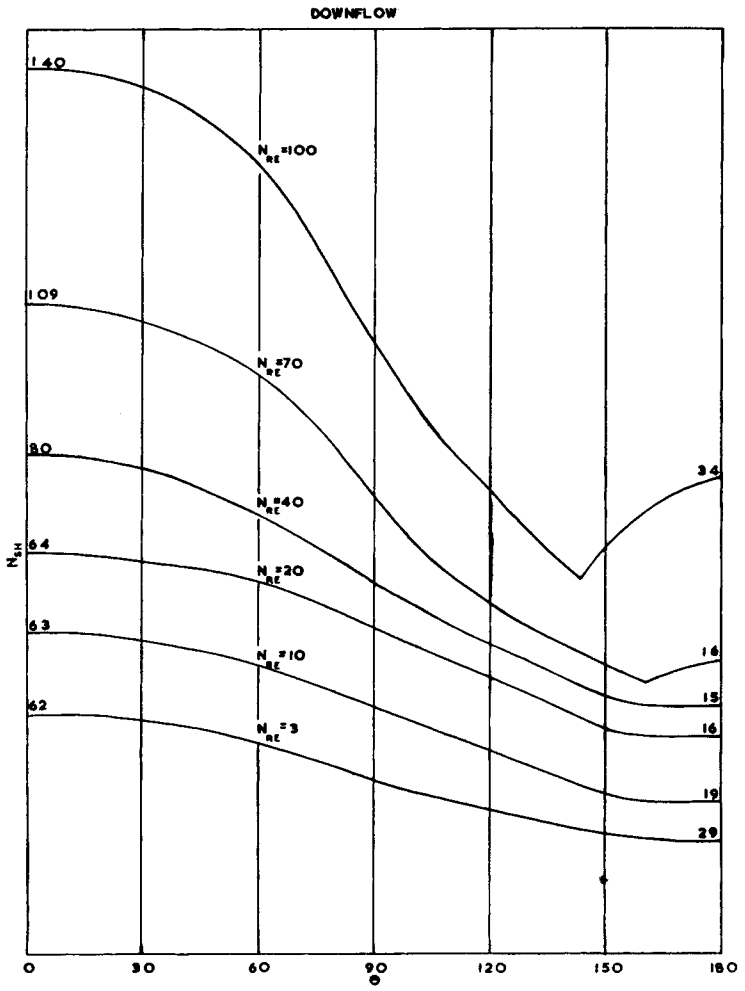

Fig. 4. Local mass transfer rates.

each size of sphere, one for upflow and one for downflow. These converge when either forced or free convection is dominant, but in the intermediate range there is a separation between the results for upflow and downflow. The behavior of the curves when forced or free convection is dominant, that is at very high or very low Reynolds numbers, is as predicted by Acrivos. At high Reynolds numbers $\overline{N_{Sh}} \sim A N_{Re}^{1/2} N_{Sc}^{1/3}$ or at constant N_{Sc}, $\overline{N_{Sh}} \sim B N^{1/2}_{Re}$

$$\therefore \quad (N_{Sh})/(\sqrt{N_{Re}}) \sim \text{constant.}$$

Thus at high Reynolds numbers the curves tend towards a constant value. At very low Reynolds numbers (high values of N'_{Gr}/N^2_{Re}) the curves will tend to infinity. The method suggested by Krischer and Loos (*9, 10*), involving the use of an equivalent Reynolds number, assumes that free and forced convective effects are additive. This is contradicted by the present results and the theoretical predictions of Acrivos (*1*).

The transition from forced to free convection can be seen when local mass transfer rates are plotted against Reynolds number with θ as parameter. In particular it can be seen that the mass transfer rate over the rear of the sphere is severely suppressed in downflow. These curves are of similar form for both sizes of sphere.

The transition can be illustrated more clearly by plotting N_{Sh} vs. θ with N_{Re} as parameter (Figures 3 and 4). The numbers on the left and right sides of each curve represent the Sherwood numbers at the front and rear stagnation points respectively and give an indication of the scale. For upflow it can be seen that as the flow is decreased, the distribution of mass transfer over the sphere surface becomes more uniform and the position of minimum transfer moves forward at low Reynolds numbers. The pattern of transfer thus tends toward that due to free convection. In downflow on the other hand it can be seen that the position of minimum transfer is moved back towards the rear stagnation point and transfer in this region is very low. Once again at low flow rates the distribution of transfer becomes similar to that due to free convection.

In Figure 5 the angle of the minimum mass transfer rate, which corresponds approximately to the point of separation of forward flow, is compared with the position of separation of forward flow, obtained under conditions of no mass transfer (*6*). For upflow at low Reynolds numbers the separation angle is markedly affected by gravitational forces, but the effect is less for downflow and for the smaller sphere. For upflow free convective forces tend to enlarge the wake, and for downflow they tend to inhibit its formation. This behavior has been predicted theoretically (*1*).

The interaction between forced and free convection is complex and can best be illustrated by considering the

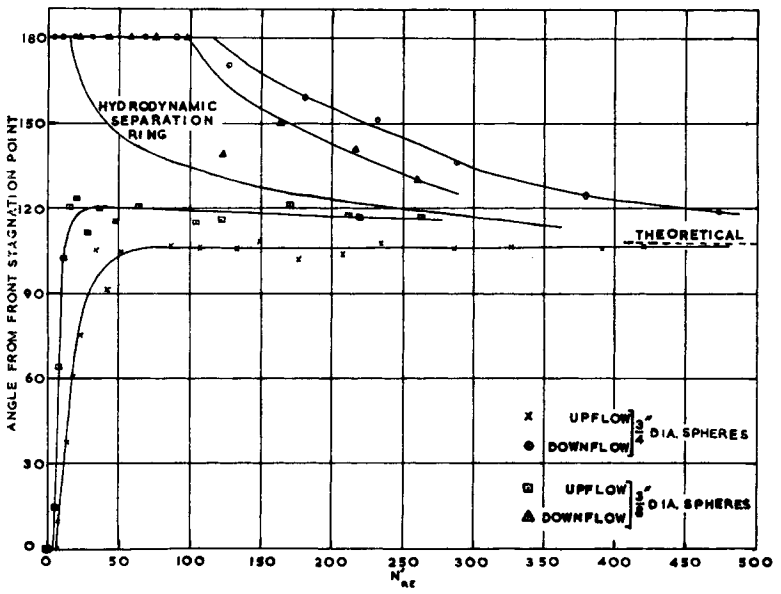

Fig. 5. Angle of minimum mass transfer.

respective flow patterns (Figure 7). For upflow, free and forced convective currents will aid each other in the main stream but will oppose near the surface of the sphere in front of the wake. In the wake itself however free and forced convective effects aid each other. At low flow rates this brings the separation point forward, as has been shown by the experimental results.

For downflow, free and forced convection oppose in the main stream but unite near the surface of the sphere forward of the wake. In the wake itself free convection opposes circulation, and this is corroborated by plots of local mass transfer coefficients around the surface of the sphere which show mass transfer in the wake to be severely suppressed in downflow. This would seem to be the major reason for upflow transfer rates being greater than downflow rates over the region of interference.

In the region of transition from forced to free convection the flow pattern does not appear to be very stable, particularly for upflow. In this case the separation angle is greater and the wake is larger than that due to hydrodynamic effects alone. It is held in place by the solute dissolved in it. For upflow at low Reynolds numbers it can also be seen from Figure 5 that the separation angle changes very rapidly with Reynolds number. Thus small changes in concentration and flow would cause the wake to oscillate. Similarly in downflow, circulation in the wake ceases well before it should because of the slowing down of the flow alone, due entirely to the weight of the solute. This can be seen in photographs obtained in this region with dye-coated spheres which showed an instability in flow (*6*). Free convection has also been shown to cause instability in flow for heat transfer at low Reynolds numbers in vertical tubes, both for upflow and downflow (*8*).

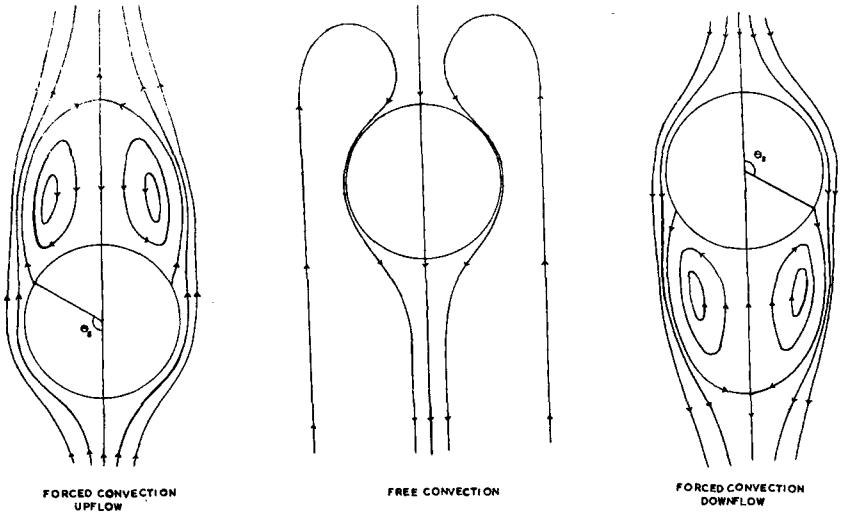

Fig. 7. Convective flow patterns

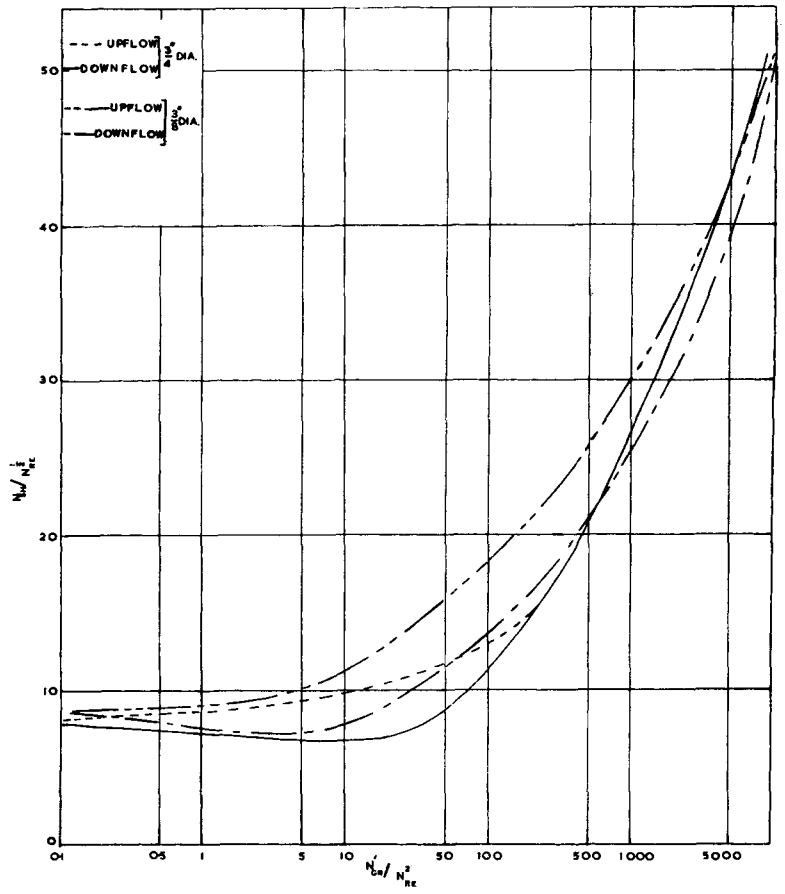

Fig. 6. Over-all mass transfer rates.

NOTATION

A	= constant	
B	= constant	
c	= concentration	Mc^{-3}
c_s	= concentration at sphere surface	
c_o	= concentration at outer edge of boundary layer	
D	= diffusivity	L^2T^{-1}
d	= sphere diameter	L
f	= function sign	
g	= gravitational acceleration	LT^{-2}
h	= diminution of radius	L
k	= thermal diffusivity	L^2T^{-1}
k_L	= mass transfer coefficient	LT^{-1}
p	= pressure	$ML^{-1}T^2$
r	= distance radially from sphere	L
t	= time interval	T
T	= temperature	θ
ΔT	= temperature difference	θ
u	= velocity parallel to surface	LT^{-1}
U_o	= characteristic velocity	LT^{-1}
U^x	= velocity on outer edge of boundary layer	LT^{-1}
$U_{(x_1)}$	= velocity distribution on outer edge of boundary layer, dimensionless	
v	= velocity normal to surface	LT^{-1}
W_{max}	= free convective velocity defined in text	LT^{-1}
x	= distance coordinate along surface	L

y = distance coordinate normal to surface L

Greek Letters

α = angle of separation of forward flow

β = coefficient of cubical expansion θ^{-1}

δ = boundary layer thickness L

η = dimensionless concentration gradient defined in text

ϵ = angle between normal to surface and the vertical

θ = angle from forward stagnation point

ρ_s = solid density ML^{-3}

ρ = fluid density ML^{-3}

$\Delta\rho$ = density difference across boundary layer ML^{-3}

σ = standard deviation

ν = kinematic viscosity L^2T^{-1}

Dimensions

L = length

M = mass

T = time

θ = temperature

Dimensionless Groups

$N_{Gr} = (gd^3\beta\Delta T)/(\nu^2)$ = Grashof number for heat transfer

$N'_{Gr} = (gd^3\Delta\rho)/(\nu^2\rho)$ = Grashof number for mass transfer

$N_{Pr} = \nu/k$ = Prandtl number

$N'_{Ra} = (gd^3\Delta\rho)/(\nu^2\rho)\ \nu/D$ = Rayleigh number

N_{Re} = Reynolds number based on average duct velocity

N'_{Re} = Reynolds number based on approach velocity

$N_{Re}{}^{+}$ = equivalent Reynolds number defined in text

$N_{Re_w\,max}$ = free convective Reynolds number defined in text

$N_{Sc} = \nu/D$ = Schmidt number

$N_{Sh} = K_L d/D$ = Sherwood number

Superscribed bars indicate over-all values.

LITERATURE CITED

1. Acrivos, Andreas, *A.I.Ch.E. Journal*, 4, 285 (1958).
2. Bar-Ilan, M., and W. Resnick, *Ind. Eng. Chem.*, 49, 313 (1957).
3. Gaffney, B. J., and T. B. Drew, *ibid.*, 42, 1120 (1950).
4. Goldstein, Samuel, "Modern Developments in Fluid Dynamics," Oxford (1938).
5. Garner, F. H., and J. M. Hoffman, *A.I.Ch.E. Journal*, to be published.
6. Garner, F. H., and R. B. Keey, *Chem. Eng. Sci.*, 9, 119 (1958).
7. Garner, F. H., and R. D. Suckling, *A.I.Ch.E. Journal*, 4, 114 (1958).
8. Hanratty, T. J., E. M. Rosen, and R. L. Kabel, *Ind. Eng. Chem.*, 50, 815 (1958).
9. Krischer, O., and H. Kroll, "Die Wissenschaftlichen Grundlagen der Trocknungstechnik," p. 127 (1956).
10. Krischer, O., and G. Loos, *Chem. Ing. Technik*, 31 (1958).

Manuscript received September 9, 1959; revision received January 27, 1960; paper accepted January 29, 1960.

A Theoretical Analysis of Laminar Natural Convection Heat Transfer to Non-Newtonian Fluids

ANDREAS ACRIVOS

University of California, Berkeley, California

An equation is given for the local Nusselt number in laminar convection heat transfer to power-law non-Newtonian fluids. This expression, which even for Newtonian fluids ($n = 1$) does not appear to have been derived before, is obtained from the exact asymptotic solution of the appropriate laminar boundary layer equations and is applicable to any two-dimensional surface or a surface of revolution about an axis of symmetry when, as is usually the case, $N_{Pr} > 10$.

The increasing emergence of non-Newtonian fluids, such as molten plastics, pulps, emulsions, etc. as important raw materials and products in a large variety of industrial processes, has stimulated a considerable amount of interest in the behavior of such fluids when in motion. In particular what has been studied most intensely for obvious practical reasons is how momentum and heat are transferred to a moving non-Newtonian fluid under the more common flow configurations usually met in practice. It is understandable therefore that some of the simpler problems of classical hydrodynamics, such as pressure drop and heat transfer in pipes and channels, flow between rotating concentric cylinders, etc., have been reinvestigated by the use of many types of non-Newtonian fluids. The results of these studies are to be found in the review article by Metzner (*9*) and in some recent publications on this subject (*3, 4, 10*).

In keeping with this general trend Acrivos, Petersen, and Shah (*1*) have recently presented a theoretical analysis of forced convection momentum and heat transfer in laminar boundary-layer flows of non-Newtonian fluids past external surfaces. As is well known, laminar boundary-layer theory, in which the viscous terms of the equations of motion are retained only in a very thin region near the surface, has made possible the study of a rather general and important class of fluid mechanical systems. It appeared worthwhile therefore to extend the boundary-layer theory to non-Newtonian fluids in order to investigate even further their properties under flow conditions.

The present analysis may be considered as a direct continuation of the work reported earlier (*1*). Its purpose is to study theoretically the problem of

It is interesting to note that Equations (27) and (36) can readily be integrated over the surface to yield the average Nusselt number $N_{\overline{Nu}}$.

Thus from Equation (36)

$$N_{\overline{Nu}} \int_0^{x_1} r_1\,dx_1 = -\theta'(0)\left(\frac{3n+1}{2n+1}\right)^{\frac{2n+1}{3n+1}} N_{Gr}^{\frac{1}{2(n+1)}} N_{Pr}^{\frac{n}{3n+1}} \left[\int_0^{x_1} r_1^{\frac{3n+1}{2n+1}} (\sin\epsilon)^{\frac{1}{2n+1}}\,dx_1\right]^{\frac{2n+1}{3n+1}}$$